HAL open science

Magnetic order suppression and structural characterization of MnNb 2 - x V x O 6 columbites crystallized under extreme pressure conditions

M.L. Hneda, J.B.M. da Cunha, A. Popa, O. Isnard

▶ **To cite this version:**

M.L. Hneda, J.B.M. da Cunha, A. Popa, O. Isnard. Magnetic order suppression and structural characterization of MnNb 2 - x V x O 6 columbites crystallized under extreme pressure conditions. Journal of Magnetism and Magnetic Materials, 2020, 496, pp.165907. 10.1016/j.jmmm.2019.165907 . hal-03488742

HAL Id: hal-03488742

https://hal.science/hal-03488742v1

Submitted on 20 Jul 2022

HAL is a multi-disciplinary open access archive for the deposit and dissemination of scientific research documents, whether they are published or not. The documents may come from teaching and research institutions in France or abroad, or from public or private research centers.

L'archive ouverte pluridisciplinaire **HAL**, est destinée au dépôt et à la diffusion de documents scientifiques de niveau recherche, publiés ou non, émanant des établissements d'enseignement et de recherche français ou étrangers, des laboratoires publics ou privés.

Distributed under a Creative Commons Attribution - NonCommercial 4.0 International License

Version of Record: https://www.sciencedirect.com/science/article/pii/S0304885319314143
Manuscript_7db7f74b7f9287261bb54dd8cef9f564

Magnetic order suppression and structural characterization of $MnNb_{2-x}V_xO_6$ columbites crystallized under extreme pressure conditions

M. L. Hneda[a,b,e], J. B. M. da Cunha[b], A. Popa[c], O. Isnard[d,e,*]

[a] *Universidade Federal dos Vales do Jequitinhonha e Mucuri, 39447-814 Janaúba, Brazil*
[b] *Universidade Federal do Rio Grande do Sul, CP 15051, 91501-970 Porto Alegre, Brazil*
[c] *National Institute for R&D of Isotopic and Molecular Technologies, 400293 Cluj-Napoca, Romania*
[d] *CNRS, Institut Néel, 25 rue des Martyrs, BP 166, F-38042 Grenoble, France*
[e] *Université Grenoble Alpes, F-38042 Grenoble, France*

Abstract

This work presents the physical properties of unusual orthorhombic form of $MnNb_{2-x}V_xO_6$ series of compounds. Isostructural *Pbcn* samples were obtained under ambient and extreme conditions of high pressure (6.7 GPa) and high temperature. All compounds present negative Curie-Weiss temperature θ_{CW} indicating dominant antiferromagnetic interactions in paramagnetic state. Extreme compounds MnV_2O_6 and $MnNb_2O_6$ exhibits magnetic structure characterized by commensurate propagation vectors $\mathbf{k} = (0, 0, \frac{1}{2})$ and $(0, 0, 0)$, respectively. In spite of different composition and large volume difference, MnV_2O_6 and $MnNb_2O_6$ present very similar macroscopic magnetic properties. The substitution of cations on B site in AB_2O_6 provides chemical disorder and induces disappearance of magnetic ordered state for the $MnNbVO_6$ intermediate system down to 1.5 K. Specific heat measurements are presented down to $T = 1.8$ K and discussed in the light of magnetic measurements and neutron-diffraction data.

Keywords: low dimensional magnetism, neutron diffraction, chemical disorder, Heisenberg chains.

1. Introduction

The AB_2O_6 series of compounds have been extensively studied due to their very interesting magnetic properties [1–3]. In these compounds A is a divalent magnetic cation and B a non-magnetic pentavalent cation. The crystal structure depends strongly on the B ion when crystallized under normal pressure conditions. For example, B = Ta yields a tetragonal structure [1] while Nb favors an orthorhombic one [2, 4]. Under high pressure, different polymorphs can be obtained [5, 6], presenting different physical properties as magnetic, electric, etc.

Under ambient pressure, MnV_2O_6 crystallizes in monoclinic structure with space group *C2/m* [3, 7, 8]. The monoclinic form having a transition to an ordered state without the low-dimensional magnetic behavior [3]. On the contrary, $MnNb_2O_6$ orders magnetically [9], exhibiting low-dimensional behavior, due to weakly interacting one-dimensional magnetic chains. Under high pressure and high temperature, MnV_2O_6 suffers a transformation from monoclinic *C2/m* to a more symmetric orthorhombic *Pbcn* structure [5]. This transformation involves an increase of vanadium coordination from 5+1 to 6, followed by a change in oxygen packing from cubic to hexagonal close-packed and a retention of a part of the VO_6 sheets, as well as a collapse of AO_6 rutile-like chains into α-PbO_2-like chains [5]. In *Pbcn* structure, the Mn^{2+} and Nb^{5+} (or V^{5+}) are located at *4c* and *8d* positions, respectively. Orthorhombic isostructural $MnNb_2O_6$ and MnV_2O_6 were found to undergo a transition from a paramagnetic phase to an ordered structure [4, 9–11] at 4.4 and 4.7 K, respectively. For these compounds ($x = 0$ and 2), Mn^{2+} cations in the octahedral site forms ferromagnetic zig-zag chains running along the c-axis in a triangular lattice arrangement in the basal ab plane.

We have recently reported [11, 12] results on

*Corresponding author
Email address: olivier.isnard@neel.cnrs.fr (O. Isnard)

© 2019 published by Elsevier. This manuscript is made available under the CC BY NC user license
https://creativecommons.org/licenses/by-nc/4.0/

the $Mn(Nb,V)_2O_6$ series of compounds, characterized by low-dimensional magnetic behavior. Our group has worked on the systems with mixture of cations in the site A and B in order to understand these influences on the crystallographic and magnetic structures. For example, extreme orthorhombic compounds $MnNb_2O_6$ and MnV_2O_6 present interesting magnetic structure characterized by commensurate propagation vectors $\mathbf{k} = (0, 0, 0)$ and $(0, 0, \frac{1}{2})$, respectively. In spite of different composition and large volume difference, these compounds present very similar macroscopic magnetic properties. Under ambient pressure, the solubility limit of V is very low in substitution $MnNb_{2-x}V_xO_6$, being about $x = 0.2$ for a single orthorhombic phase [12]. In this work we present a detailed investigation of orthorhombic *Pbcn* $MnNb_{2-x}V_xO_6$ ($x = 0$, 1 and 2) compounds by means of powder neutron and X-ray diffraction measurements, specific-heat and magnetic measurements. This study is aimed to investigate the effect of B-site ion substitution on the structural and magnetic properties of columbite compounds obtained under ambient ($x = 0$) and extreme conditions ($x = 1$ and 2) of high temperature and high-pressure.

2. EXPERIMENTAL DETAILS

Samples were prepared with appropriate amounts of Mn acetate ($C_4H_6MnO_4{\cdot}4H_2O$), MnO, V_2O_5 and Nb_2O_5, from Sigma-Aldrich with purity of $\geq 99\%$, 99%, $\geq 99.6\%$ and 99.99%, respectively. The mass of powders were previously obtained, then mixed and ground using an agate mortar during one hour to homogenize the mixture. After that, the mixtures were pressed into pellets and heat-treated in air during different temperatures and times (with powder homogenization and pressed into pellets between each heat treatment), as follows: $MnNb_2O_6$ was subjected to following treatments: 673, 923, 1000 and 1373 K for 12, 16, 48 and 36 h respectively, and presented orthorhombic *Pbcn* structure. MnV_2O_6 sample synthesis began from the standard monoclinic material obtained at ambient pressure under following heat treatments: 673, 923, 1000 K for 12, 16, and 48 h, respectively. Another treatment at 1000 K for 48 h was made, followed by a quenching in N_2. Then a high pressure and high-temperature treatment (6.7 GPa, 1073 K for 1 h), using a belt press (Institut Néel/CNRS - Grenoble), was performed and the MnV_2O_6 presented an orthorhombic *Pbcn* space-group symmetry. The $MnNbVO_6$ was obtained from $MnNb_2O_6$ and MnV_2O_6 phases. The appropriate mixture was submitted to a high pressure high-temperature treatment (5 GPa, 1083 K) for 1 h. Sample purity was first checked by XRD analysis at room temperature followed by neutron diffraction (ND) and magnetic measurements. The XRD was performed in transmission geometry, using Cu Kα radiation, $\lambda(K_{\alpha 1}) = 1.540562$ Å, with a scan step of 0.05° and angular 2θ range from 20° to 80°.

Neutron diffraction patterns were recorded with the double-axis high-flux diffractometer D1B. This line is operated by the CNRS at the Institut Laue-Langevin (ILL), Grenoble, using a 2.52 Å wavelength selected by a pyrolytic graphite monochromator. This is a powder diffractometer operating with a take-off angle of the monochromator of 44° (in 2θ). In this configuration the multicounter is composed of 1280 cells covering a total angular domain of 128° (in 2θ), with a detector step of 0.1°. ND measurements were performed using a vanadium sample holder.

Structural refinements with Rietveld method was made for XRD and ND data (to extract the crystallographic and magnetic parameters) with FULLPROF package [13]. Agreement factors are defined according to the guidelines of the Rietveld refinement [14] as described elsewhere.

Magnetic measurements were undertaken on powder samples in the temperature range from 1.9 to 300 K, using a SQUID magnetometer. Isothermal magnetization curves were recorded in applied magnetic fields ranging from 0 to 50 kOe, and the thermal dependence of magnetic susceptibility was measured in fields of 50 and 10 Oe.

Specific heat measurements were performed on pellets (mass $\sim$ 5 mg), using a PPMS (Physical Property Measurement System - Quantum Design), with the temperature relaxation method in the range of 1.8-300 K. This method consists in increasing the sample temperature with a known power and then fitting the temperature relaxation during heating and cooling.

EPR measurements were carried out in the temperature range 110-350 K using a X-band (9.52 GHz) Bruker ELEXSYS 500 spectrometer equipped with a continuous nitrogen flow cryostat. The EPR spectra processing was performed by Bruker Xepr software.

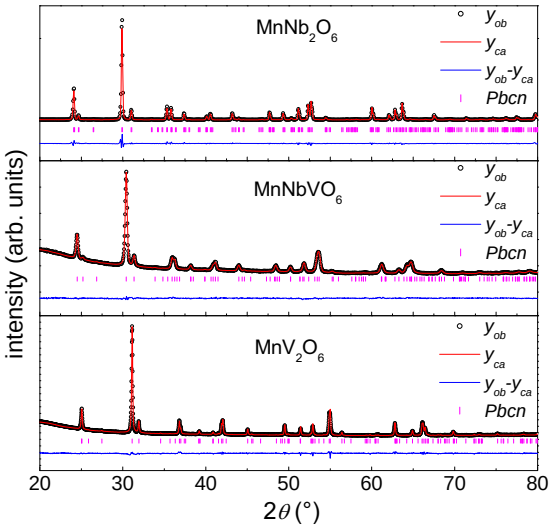

Figure 1: Rietveld refinement of the X-ray diffraction (λ = 1.540562 Å) pattern recorded at room temperature for $MnNb_{2-x}V_xO_6$ columbites (x = 0, 1 and 2). For all compounds, the Bragg positions correspond to the *Pbcn* space group, as indicated. y_{ob} and y_{ca} are the observed and calculated intensities, respectively.

3. RESULTS AND DISCUSSION

3.1. X-ray diffraction

The $MnNb_{2-x}V_xO_6$ columbites synthesis was obtained at ambient and high-pressure and high-temperature treatments, as described in experimental details session. After the different routes, all samples presented single phase with the orthorhombic structure - *Pbcn* space-group symmetry. Figure 1 shows the Rietveld analysis of the XRD pattern recorded at room temperature for the orthorhombic form. It can be seen from the patterns and refinement that all samples present no evidence of spurious reflections related to different phases. This feature is well seen in Fig. 1 in which the experimental XRD pattern (empty circles) for x = 0, 1 and 2 is reported together with the calculated profile (red line). The difference between observed and calculated pattern is shown as a blue line at the bottom of each measurement; the theoretical Bragg peaks for the columbite phase are represented by vertical magenta lines. Table 1 shows the room temperature XRD parameters for $MnNb_{2-x}V_xO_6$ columbites (x = 0, 1 and 2): atomic positions, cell parameters and agreement factors $R_{\rm wp}$ and R_B of the Rietveld refinement.

Table 1: Structural parameters obtained from X-ray powder diffraction (λ = 1.540562 Å) at room temperature for $MnNb_{2-x}V_xO_6$ columbites in *Pbcn* space group (x = 0, 1 and 2).

		$MnNb_2O_6$	$MnNbVO_6$	MnV_2O_6
	x	0	0	0
Mn	y	0.180(3)	0.190(2)	0.196(1)
	z	0.25	0.25	0.25
	x	0.1626(3)	0.1633(4)	0.1698(4)
Nb/V	y	0.3188(9)	0.322(1)	0.3202(9)
	z	0.760(2)	0.756(2)	0.753(2)
	x	0.102(2)	0.100(1)	0.0967(6)
O1	y	0.412(5)	0.415(4)	0.413(2)
	z	0.445(7)	0.411(4)	0.434(3)
	x	0.083(2)	0.083(7)	0.0996(8)
O2	y	0.127(6)	0.119(4)	0.148(2)
	z	0.888(7)	0.951(4)	0.863(3)
	x	0.253(3)	0.247(1)	0.263(1)
O3	y	0.127(6)	0.155(4)	0.120(3)
	z	0.586(6)	0.625(4)	0.597(5)
a (Å)		14.431(1)	14.132(2)	13.7722(7)
b (Å)		5.7638(4)	5.700(1)	5.6004(3)
c (Å)		5.0820(4)	4.9928(8)	4.8779(3)
vol. (Å^3)		422.73(5)	402.2(1)	376.24(4)
$R_{\rm wp}$ (%)		15.2	9.2	8.1
R_B (%)		4.8	5.8	6.6

It is observed a volume reduction of 11% between the extreme isostructural orthorhombic compounds, $MnNb_2O_6$ and MnV_2O_6, the latter being the smaller one. For the cell parameters, a reduction of 4.6%, 2.8% and 4.0% is observed for *a*, *b* and *c* axes, respectively. As expected, $MnNbVO_6$ presents parameters between the extreme compounds. The variations of these parameters are shown in Figure 2, where it is possible to observe the Vegard's law.

3.2. Neutron diffraction

Neutron-diffraction measurements for $MnNbVO_6$ were carried out at different temperatures, since differences in diffractograms can reveals some long distance magnetic ordering or even short-range magnetic correlations. Rietveld refinement of the ND pattern ($\lambda = 2.52$ Å) is shown in Fig. 3, taken at 20 and 1.5 K, respectively. Refinement of the diffraction pattern demonstrates that the crystal structure remains the same, but the diffraction pattern does not exhibit extra reflections that could be related to magnetic order at very low temperatures. Table 2 presents the structural parameters obtained from neutron powder diffraction ($\lambda = 2.52$ Å) with Rietveld refinement at 20 K and 1.5 K for orthorhombic $MnNb_{2-x}V_xO_6$ columbites ($x = 0$, 1 and 2). In these Rietveld refinements, the (x, y, z) atomic-positions parameters of vanadium were constrained to those derived from XRD due to the almost null neutron coherent scattering factor of V atom. Since ND is more sensitive to light atoms, such as oxygen, this structural refinement confirms unambiguously that the oxygen octahedra are packed following the *Pbcn* crystal symmetry. The non-indexed peak around $2\theta = 72°$ is due to diffraction of vanadium sample holder and cryostat tail.

The crystalline structure of $MnNb_{2-x}V_xO_6$ orthorhombic *Pbcn* compounds highlighting the zigzag chains running along the *c*-axis is shown in Figure 4. These chains are formed by oxygen octahedra surrounding the Mn atoms and are disposed in a triangular network in *ab* plane. For extreme compounds ($x = 0$ and 2), at 1.5 K, the magnetic structure is commensurable with the lattice and presents a propagation vector $\mathbf{k} = (0, 0, 0)$ and $(0, 0, \frac{1}{2})$ for $MnNb_2O_6$ and MnV_2O_6, respectively. For MnV_2O_6 magnetic moments are mainly lying in the *bc* plane forming a + + - - configuration [11] whereas in $MnNb_2O_6$ compound exhibits AF zigzag chains forming + - + - spin sequence, running along the *c*-axis [12]. These chains are schematically represented on the right of Fig. 4.

3.3. Magnetic measurements

The temperature dependence of the *dc* susceptibility for $MnNb_{2-x}V_xO_6$ columbites is shown in Fig. 5. All measurements were performed in field cooling mode (FC). Looking closely around the observed peak for extreme compositions ($x = 0$ and 2), one sees that it is not sharp, but rather broad, a feature typical of low-dimensional magnetism. These compounds, with *Pbcn* crystal structure symmetry and octahedral chains, exhibits characteristic features of low-dimensional magnetism, similarly to what was observed in other isostructural ANb_2O_6 compounds A = Fe, Ni and Co [15–20]. The Néel temperature corresponds to an inflection point slightly below the maximum [21]. Contrary to compounds with $x = 0$ and 2 which present a drop of the susceptibility at low temperature, the $MnNbVO_6$ compound does not present any sign of magnetic transition, there is no maximum in the susceptibility at temperatures higher than 1.7 K. This result confirms the absence of magnetic peaks on the neutron diffraction pattern. It is not clear at present if any order will appear at much lower temperature, the Nb,V cation disorder contributes to the disappearance of long range magnetic order for $MnNbVO_6$ or at least to the observed large reduction of the ordering temperature if any order appears at lower temperature. Complementary specific heat measurements will be discussed later on.

The paramagnetic susceptibility as a function of temperature was fitted to the Curie-Weiss law, $\chi(T) = C/(T - \theta_{CW})$, where C is the Curie constant and θ_{CW} the Curie-Weiss temperature. Figure 6 shows the reciprocal susceptibility with the corresponding fit for $MnNbVO_6$. The parameters of $MnNb_{2-x}V_xO_6$ obtained from this analysis are listed in Table 3. The effective magnetic moment in the paramagnetic state has been derived from the Curie constant. It is worth to point out the importance of the structure in the magnetic behavior; these compounds have crystal-structure geometry common, in particular the existence of octahedral chains of Mn located on a triangular net. MnV_2O_6 and $MnNb_2O_6$ columbites present very similar T_N besides the fact that the MnV_2O_6 presents a much reduced unit cell, compared to $MnNb_2O_6$ one.

Mn^{2+} cations are in the $^6S_{5/2}$ electronic state in $MnNb_{2-x}V_xO_6$ compounds. The calculated value of effective magnetic moment, given by $\mu_{\text{eff}} =$

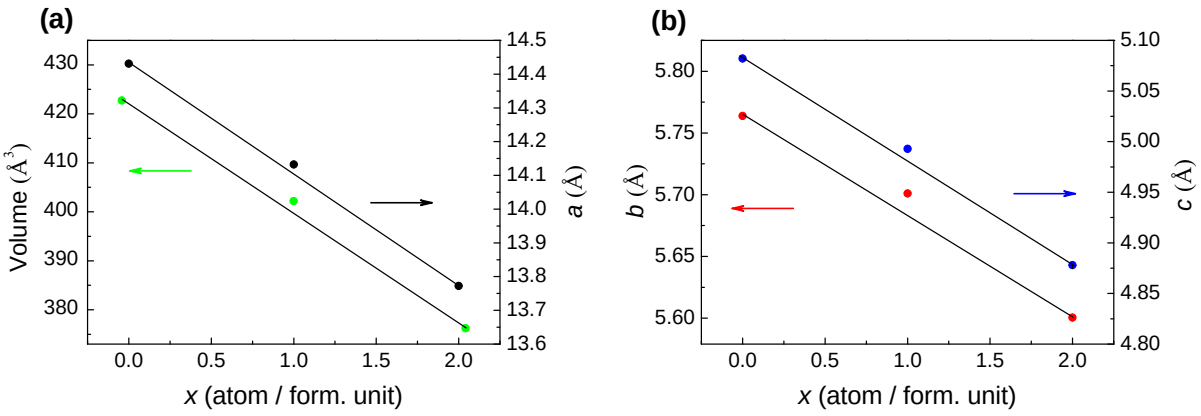

Figure 2: Room temperature unit-cell parameters comparison for $MnNb_{2-x}V_xO_6$ columbites (x = 0, 1 and 2).

Table 2: Structural parameters obtained from neutron powder diffraction (λ = 2.52 Å) at 20 K and 1.5 K for $MnNb_{2-x}V_xO_6$ columbites (x = 0, 1 and 2).

		$MnNb_2O_6$		$MnNbVO_6$		MnV_2O_6	
Temperature		20 K	1.5 K	20 K	1.5 K	20 K	1.5 K
	x	0	0	0	0	0	0
Mn	y	0.183(4)	0.165(3)	0.15(1)	0.16(1)	0.170(6)	0.183(4)
	z	0.25	0.25	0.25	0.25	0.25	0.25
	x	0.1598(4)	0.1600(4)	0.1633	0.1633	0.1698	0.1698
Nb/V	y	0.310(1)	0.315(1)	0.322	0.322	0.3202	0.3202
	z	0.758(1)	0.763(2)	0.756	0.756	0.753	0.753
	x	0.094(1)	0.0954(6)	0.097(2)	0.096(2)	0.095(1)	0.0947(9)
O1	y	0.392(2)	0.400(2)	0.414(6)	0.407(6)	0.403(3)	0.400(2)
	z	0.439(2)	0.438(2)	0.446(6)	0.446(6)	0.465(3)	0.462(2)
	x	0.082(1)	0.0817(6)	0.081(2)	0.084(2)	0.087(1)	0.0875(9)
O2	y	0.109(2)	0.109(2)	0.111(6)	0.103(4)	0.109(3)	0.112(2)
	z	0.900(2)	0.902(2)	0.892(8)	0.882(6)	0.895(3)	0.895(2)
	x	0.254(1)	0.2541(7)	0.255(3)	0.262(2)	0.255(1)	0.2560(9)
O3	y	0.126(2)	0.128(2)	0.134(7)	0.129(8)	0.143(3)	0.140(2)
	z	0.585(2)	0.585(2)	0.58(1)	0.57(1)	0.605(4)	0.607(3)
a (Å)		14.411(2)	14.414(2)	14.131(6)	14.133(6)	13.761(4)	13.7580(8)
b (Å)		5.7577(8)	5.7571(6)	5.688(1)	5.688(1)	5.589(2)	5.5889(4)
c (Å)		5.0775(7)	5.0775(5)	4.994(2)	4.995(2)	4.881(2)	4.8805(4)
Volume (Å^3)		421.3(1)	421.35(9)	401.5(2)	401.6(2)	375.4(2)	375.28(5)
R_{wp} (%)		13.4	4.5	21.6	21.7	4.0	2.7
R_B (%)		9.7	6.4	18.7	18.3	9.3	5.6
R_M (%)		-	9.4	-	-	-	12.7
μ (μ_B)		-	4.13(6)	-	-	-	3.76(5)

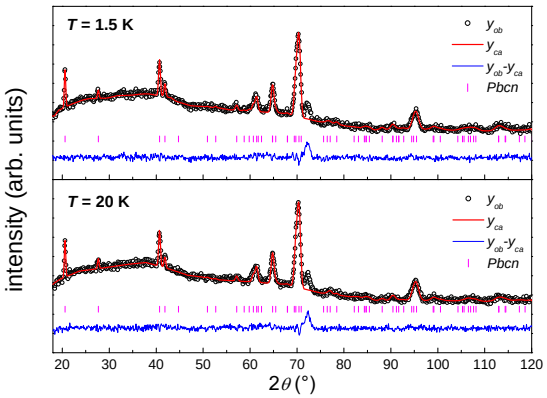

Figure 3: ND measurements for $MnNbVO_6$ showing a very similar pattern at 20 and 1.5 K, indicating non-magnetic order at these temperatures. The row of markers refers to Bragg-peak positions corresponding to the nuclear contribution (*Pbcn* space group). The non-indexed peak around $2\theta = 72°$ is related to the vanadium sample holder and cryostat tail. y_{ob} and y_{ca} are the observed and calculated intensities, respectively.

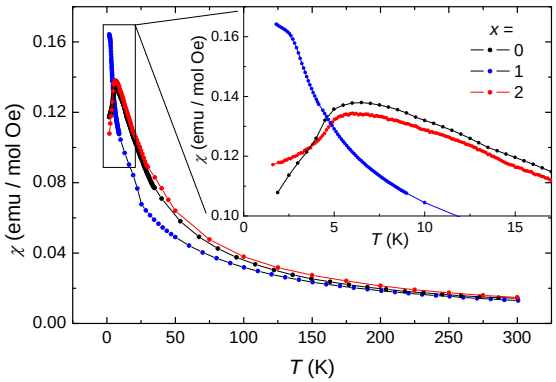

Figure 5: Comparison between $x = 0$, 1 and 2 susceptibility measurements. Notice that there is no indication of ordering for $x = 1$ down to temperatures of 1.7 K.

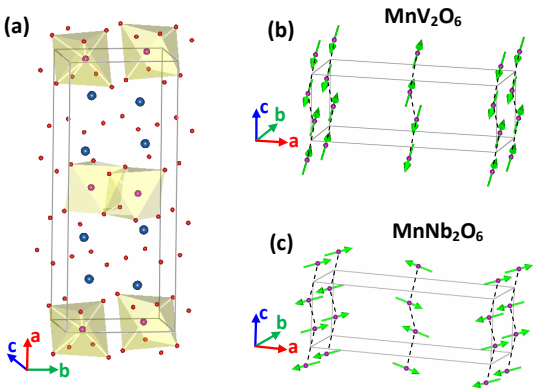

Figure 4: (a) Crystal structure of $MnNb_{2-x}V_xO_6$ compounds and oxygen (red spheres) octahedra surrounding the Mn (pink spheres) atoms, Nb/V ones are shown as blue spheres. Magnetic ordered state for the extreme compounds $x = 2$ (b) and $x = 0$ (c).

Table 3: Néel temperature (T_N), Curie-Weiss temperature (θ_{CW}), Curie constant (C - *measured in emu K/mol Oe), effective magnetic moment and frustration index ($f = |\theta_{CW}|/T_N$) of $MnNb_{2-x}V_xO_6$ samples obtained from measurements of *dc* susceptibility.

	$MnNb_2O_6$	$MnNbVO_6$	MnV_2O_6
T_N (K)	4.4	-	4.7
θ_{CW} (K)	-24.5	-40.4	-24.6
C (*)	4.78	4.46	4.46
μ_{eff} (μ_B)	6.2	6.0	6.0
f	5.6	$\rightarrow \infty$	5.2

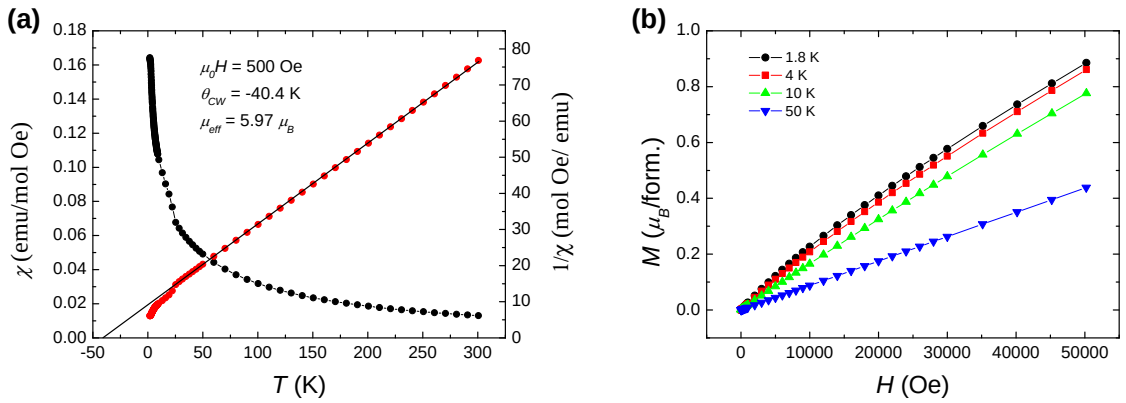

Figure 6: (a) Susceptibility measurement and reciprocal susceptibility for $MnNbVO_6$ showing no magnetic order down to 1.5 K. (b) Isothermal magnetization curves recorded at the indicated temperatures.

$g\mu_B[S(S+1)]^{1/2}$ [4], is 5.92 μ_B for $g = 2$ and $S = 5/2$. This value is quite close to the one obtained here from susceptibility measurements, as can be seen in Table 3. It has been reported a value of $\mu_{\text{eff}} = 5.91$ μ_B for the $MnNb_2O_6$ compound in the literature [22]. The obtained value of μ_{eff} confirms the divalent state of Mn in the studied compounds. It also shows that orbital effects are essentially absent and it should not be expected an Ising-like behavior with strong anisotropy, as reported previously for other columbites (Co/Fe)Nb_2O_6 [18, 19]. It is also interesting to remark a negative Curie-Weiss temperature for these phases, MnV_2O_6 presented a θ_{CW} = -24.6 K, very close to that of $MnNb_2O_6$ (-24.5 K), $MnNbVO_6$ presented a θ_{CW} = -40.4 K. This temperature indicates that the similitude between these materials observed in the ordering is well reflected in the paramagnetic state. This indicates that the dominant exchange interactions are antiferromagnetic, and testifies the important role of the crystal structure in determining the exchange interactions operating in the $MnNb_{2-x}V_xO_6$ compounds. In $MnNb_2O_6$ antiferromagnetic chains are observed. Both the larger negative value of θ_{CW} and the reduction of the ordering temperature below 1.5 K in $MnNbVO_6$ are illustrating the enhanced frustration of the AF exchange interaction in this compound.

The isothermal magnetization curves recorded at the indicated temperatures for $MnNbVO_6$ are gathered in figure 6. The phase behavior is typical of antiferromagnetic ordering, and no spin-flip transition is observed (below the order temperature) up to $\mu_0 H = 5$ kOe in contrast to other ANb_2O_6 orthorhombic systems (A = Fe, Co and Ni), which present ferromagnetic chains and show spin-flip transitions [18, 20]. This $MnNbVO_6$ compound exhibits only a spin-flop-type behavior upon increasing the intensity of applied magnetic field below T_N, which indicates a dominance of AF coupling between neighboring Mn^{2+} magnetic moments.

As it is observed, the mixed compound $MnNbVO_6$ presents very different magnetic behavior, with no magnetic ordered state down to 1.7 K, besides the fact of very similar crystal structures. In this *Pbcn* orthorhombic form, a Mn^{2+} and $(Nb/V)^{5+}$ cation are located at the center of an oxygen octahedron; with three pairs of Mn-O and six different values for B-O bonds, as summarized in Table 4 and 5. A schema of such octahedra is shown in Fig. 7. Structural data in Table 5 allow us to observe changes in the distortion of octahedral environments. It is presented the distances between the Nb/V (B-site) to six O atoms forming the octahedron. Tealdi *et al.* [23] defined the distance between cation and the barycentre of octahedron as the octahedral distortion since deviation of the cation position from the barycentre results in different cation-oxygen distances and in the deviation of the octahedral angles from the ideal value of 90°. They have concluded that B site is more distorted than the A site in $Fe_xMn_{1-x}Nb_2O_6$ columbites, probably as a consequence of the high charge of niobium cation.

It could be expected a Heisenberg-like behavior for $MnNbVO_6$, very similar to that presented by

Table 4: Distances (Å) and angles (°) of Mn to oxygens obtained from the Rietveld refinement of XRD data, label a to f (fig. 7) for $MnNb_{2-x}V_xO_6$ compounds. The distance of Mn to O-a is labelled as Mn-a.

x	Mn-a/Mn-f	Mn-b/Mn-e	Mn-c/Mn-d	Mn-Mn	a-Mn-b	c-Mn-d	e-Mn-f	Mn-O-Mn
0	2.26	2.23	2.22	3.281	164.9	164.5	164.9	94.2
1	2.35	2.08	1.94	3.312	166.6	155.6	166.6	100.5
2	2.43	2.02	2.35	3.282	162.6	166.6	162.6	86.8

Table 5: Distances (Å) and angles (°) of Nb/V (B) to oxygens obtained from the Rietveld refinement of XRD data, label a to f (fig. 7) for $MnNb_{2-x}V_xO_6$ compounds.

x	B-a	B-b	B-c	B-d	B-e	B-f	a-B-b	c-B-d	e-B-f	B-O-B
0	1.72	2.33	1.90	2.08	2.02	1.97	169.2	154.0	161.9	144.4
1	2.00	2.23	1.89	2.37	1.90	1.67	160.1	163.2	160.8	110.7
2	1.92	1.95	1.47	2.07	2.00	1.86	154.2	165.0	166.2	107.3

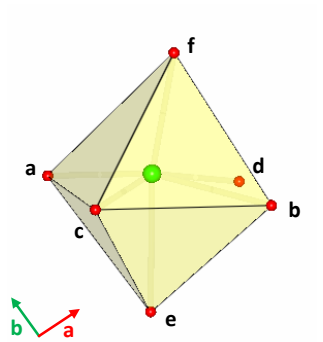

Figure 7: Oxygen (red spheres - label a to f) octahedra surrounding the Mn (green sphere) atoms for $MnNb_{2-x}V_xO_6$ compounds. A comparison of distances and angles is shown in Table 4 and 5.

$MnNb_2O_6$, relied to the *Pbcn* structure, since it has the same feature zig-zag chains of MnO_6 edge-sharing octahedra running along the c axis. Superexchange occurs through Mn-O-Mn bonds, there are two such bonds, through two oxygens at the vertices of a shared edge making angles of 94.2 and 86.8° for ordered compounds $MnNb_2O_6$ and MnV_2O_6, respectively. $MnNbVO_6$ presents a bigger Mn-O-Mn angle, 100.5° (Table 4). According to the Goodenough-Kanamori rules [24], such near-90° bond angles should yield (weak) ferromagnetic (FM) superexchange within a chain, involving t_{2g} orbitals. This bond angle is slightly larger in the $MnNbVO_6$, but still closer to 90° than to 180°. As a consequence the negative values of θ_{CW} observed in the series $MnNb_{2-x}V_xO_6$ seem to be due to interchain AF couplings, possibly a direct Mn-Mn exchange through e_g orbitals. This behavior of magnetic properties probably arises from the induced cationic disorder as well as the magnetic anisotropy of Mn^{2+} ion, which presents majoritarian spin contribution to magnetic moment. Also, this structure featuring 1D chain provides the existence of competing antiferromagnetic interactions within nearly triangular net of chains.

From a point of view of the magnetic frustration, the frustration index is defined as a ratio between the Curie-Weiss and order temperatures: $f = |\theta_{CW}|/T_N$. Such index has been calculated for the investigated compounds and listed in Table 3. It is common to consider that when the f-value is about 5 or bigger, the system can be

considered frustrated [25]. From our experimental data we obtain $f = 5.6$ and 5.2 for $MnNb_2O_6$ and MnV_2O_6 phases, respectively. The $MnNbVO_6$ presents an f index that $\rightarrow \infty$, once it is not observed a T_N at finite temperature. It is interesting to notice that, as discussed above, these orthorhombic *Pbcn* compounds present chains of Mn octahedra located on a triangular net. Such topology can indeed lead to significant frustration between the chains as long as antiferromagnetic interactions are involved. $MnNb_2O_6$ and MnV_2O_6 phases present significantly large frustration index as observed in Table 3, once T_N is substantially smaller than θ_{CW}. A low T_N arises from the (quasi)low dimensionality and isotropy of the spin system, which can only order in three dimensions. Both factors, cationic disorder and the triangular array of chains, may contribute to destabilize the magnetic order.

3.4. Specific-heat measurements

The occurrence of a magnetic transition at low temperature was also checked through specific-heat measurement. Figure 8 shows the specific-heat (C_P) curve, measured down to 1.8 K. The magnetic order is characterized by a lambda-peak at the ordering temperature. The values obtained for T_N agree with those obtained by magnetic measurements (shown in Table 3), $T_N = 4.7$ K for MnV_2O_6 and 4.4 K for $MnNb_2O_6$. The evidence of no magnetic ordered state for $MnNbVO_6$ compound at higher temperatures than 1.8 K is also observed in C_P measurements, this material presents a large Schottky-type peak near 8 K. For comparison, it is also presented a C_P measurement for ZnV_2O_6, showing the lattice contribution only.

Looking at the C_P behavior of the $MnNbVO_6$, we can conclude that no tendency to magnetic order is observed down to 1.8 K, the C_P trend at low temperature may rather indicate that such compound does not order at all since the C_P curve of $MnNbVO_6$ compound tends to merge towards the ZnV_2O_6 curve instead of showing an upturn upon cooling.

3.5. EPR measurements

EPR is a highly sensitive tool to investigate the presence of paramagnetic ions providing information about their valence state and interactions. The EPR spectra of $MnNbVO_6$ sample measured in 110-350 K temperature range are showed in the Figure 9. All the spectra present a single broad

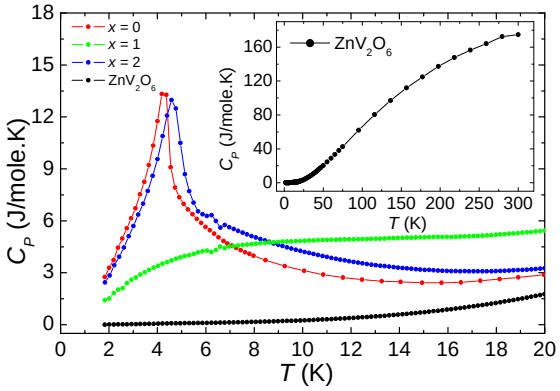

Figure 8: Specific heat measurements for $MnNb_{2-x}V_xO_6$ columbites ($x = 0$, 1 and 2). The inset shows a measurement for not magnetic ZnV_2O_6, presenting only the lattice contribution for C_P.

Lorentzian line, with the same resonance field corresponding to a $g \sim 2.006$. In the studied temperature range, no variation of resonance field with temperature was observed. Only a slight increase of the linewidth with decreasing the temperature appears as shown in the Figure 9 inset, caused by some structural adjustments [23].

In this type of compounds, the expected oxidation state of Mn ions is 2+ ($3d^5$, $S = 5/2$). Consequently, the predicted EPR spectrum consist on a specific hyperfine pattern composed of six line with $g = 2.000$ determined by the interaction of Mn^{2+} electron cloud with ^{55}Mn nucleus ($I = 5/2$). In our case, the absence of this structure is due to the large concentration of Mn^{2+} ions. The magnetic interactions between these ions lead to the line broadening [26].

Similar behavior is exhibited by $MnNb_2O_6$ and $Mn_{0.75}Fe_{0.25}Nb_2O_6$ compounds as reported in the literature [23]. The EPR parameters, g-factor and linewidth, are not influence by temperature. However, the decrease on Mn content conduct to an increase of EPR linewidth. This line broadening was attributed to the decrease of exchange interaction between Mn^{2+} ions occurred by substituting these ions with Fe^{2+}.

4. Conclusions

In this work we did a systematic study of *Pbcn* $MnNb_{2-x}V_xO_6$ compounds (with $x = 0$, 1 and 2);

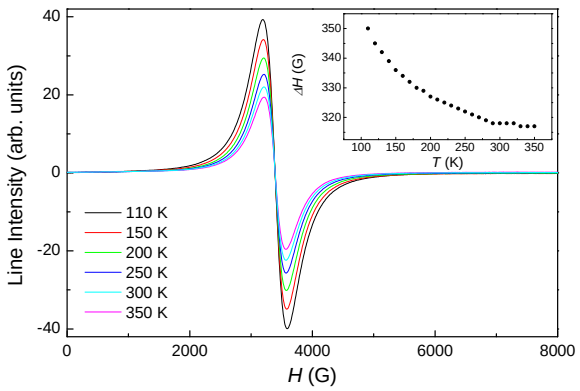

Figure 9: EPR spectrum of $MnNbVO_6$ at different temperatures. The insight shows the decrease line width ΔH as the temperature is increased.

$x = 1$ and 2 being crystallized under extreme conditions of high-pression high temperature. Susceptibility measurements of extreme compounds ($x = 0$ and 2) present a broad maximum followed by an inflection point (T_N) which characterizes low dimensional magnetic behavior. In contrast, $MnNbVO_6$ presented no long range magnetic order and its susceptibility keeps increasing at 1.7 K. For all compounds, Curie-Weiss fitting gives a negative Curie-Weiss temperature, bearing witness to the fact that the dominant exchange interactions are antiferromagnetic in paramagnetic region. Magnetization curves $M(H,T)$ for $MnNbVO_6$ vary linearly with no sharp transitions for an applied field up to 50 kOe. At 1.5 K, the $MnNbVO_6$ presents no ordered state characterized by additional magnetic peaks, with a neutron diffraction pattern very similar to that obtained at 20 K. We conclude that in spite of the fact that these compounds present very similar crystalline structure, the two extreme $MnNb_2O_6$ and MnV_2O_6 compounds are magnetically ordered at low temperature, and the substitution on B-site provides a chemical disorder inducing evolution of the system to magnetic disorder and enhanced magnetic frustration.

Acknowledgments

Funding for this project was provided by a grant from Région Rhône-Alpes (MIRA scholarship). The present work was also supported in part by the Brazilian agency CNPq and by the Brazilian-France agreement CAPES-COFECUB. The Institute Laue Langevin and the CNRS are warmly acknowledged for providing the neutron facility. The author Adriana Popa would like to express appreciation for the financial support to the Romanian Ministry of Research and Innovation project no. 32PFE/19.10.2018.

References

[1] E. J. Kinast, V. Antonietti, D. Schmitt, O. Isnard, J. B. M. da Cunha, M. A. Gusmão, C. A. dos Santos, Bicriticality in $Fe_xCo_{1-x}Ta_2O_6$, Phys. Rev. Lett. 91 (19) (2003) 197208. doi:10.1103/PhysRevLett.91.197208.

[2] S. Lee, R. K. Kaul, L. Balents, Interplay of quantum criticality and geometric frustration in columbite, Nature Physics 6 (9) (2010) 702–706. doi:10.1038/nphys1696.

[3] S. A. J. Kimber, J. P. Attfield, Disrupted antiferromagnetism in the brannerite MnV_2O_6, Phys. Rev. B 75 (2007) 064406. doi:10.1103/PhysRevB.75.064406.

[4] O. V. Nielsen, B. Lebech, F. K. Larsen, L. M. Holmes, A. A. Ballman, A neutron diffraction study of the nuclear and magnetic structure of $MnNb_20_6$, J. Phys. C 9 (12) (1976) 2401-2411. doi:10.1088/0022-3719/9/12/023.

[5] M. Gondrand, A. Collomb, J. C. Joubert, R. D. Shannon, Syntesis of new high-pressure columbite phases containing pentavalent vanadium, J. Solid State Chem. 11 (1) (1974) 1–9. doi:10.1016/0022-4596(74)90139-X.

[6] K. Mocala, J. Zilkowski, Polymorphism of the bivalent metal vanadates MeV_2O_6 (Me = Mg, Ca, Mn, Co, Ni, Cu, Zn, Cd), J. Solid State Chem. 69 (2) (1987) 299-311. doi:10.1016/0022-4596(87)90087-9.

[7] D. Hara, J. Shirakawa, H. Ikuta, Y. Uchimoto, M. Wakihara, T. Miyanaga, I. Watanabe, Charge-discharge reaction mechanism of manganese vanadium oxide as a high capacity anode material for lithium secondary battery, J. Mater. Chem. 12 (2002) 3717-3722. doi:10.1039/b206255k.

[8] Hk. Müller-Buschbaum, M. Kobel, Zur Kristallchemie von Oxovanadaten: γ-CoV_2O_6 und MnV_2O_6, J. Alloy. Compd. 176 (1) (1991) 39-46. doi:10.1016/0925-8388(91)90008-J.

[9] L. M. Holmes, A. A. Ballman, R. R. Hecker, Antiferromagnetic ordering in $MnNb_2O_5$ studied by magnetoeletric and magnetic susceptibility measurements, Solid State Commun. 11 (3) (1972) 409-413. doi:10.1016/0038-1098(72)90020-8.

[10] D. Prabhakaran, F. R. Wondre, A. T. Boothroyd, Preparation of large single crystals of ANb_2O_6 (A = Ni, Co, Fe, Mn) by the floating-zone method, J. Crys. Growth 250 (1) (2003) 72-76. doi:10.1016/S0022-0248(02)02229-7.

[11] M. L. Hneda, J. B. M. da Cunha, M. A. Gusmão, S. R. Oliveira Neto, J. Rodríguez-Carvajal, O. Isnard, Low-dimensional magnetic properties of orthorhombic MnV_2O_6: A nonstandard structure stabilized at high pressure, Phys. Rew. B 95 (2016) 024419. doi:10.1103/PhysRevB.95.024419.

[12] M. L. Hneda, J. B. M. da Cunha, M. A. C. Gusmão, O. Isnard, Low dimensional magnetism in

$MnNb_{2-x}V_xO_6$, Mater. Res. Bull. 74 (2016) 169-176. doi:10.1016/j.materresbull.2015.10.030.

[13] J. Rodríguez-Carvajal, Recent advances in magnetic structure determination by neutron powder diffraction, Phys. B 192 (1-2) (1993) 55-69. doi:10.1016/0921-4526(93)90108-I.

[14] L. B. McCusker, R. B. Von Dreele, D. E. Cox, D. Louër, P. Scardi, Rietveld refinement guidelines, J. Appl. Crystallogr. 32 (1) (1999) 36-50. doi:10.1107/S0021889898009856.

[15] C. Heid, H. Weitzel, P. Burlet, M. Bonnet, W. Gonschorek, T. Vogt, J. Norwig, H. Fuess, Magnetic phase diagram of $CoNb_2O_6$: a neutron diffraction study, J. Magn. Magn. Mater. 151 (1995) 123-131. doi:10.1016/0304-8853(95)00394-0.

[16] S. Kobayashi, S. Mitsuda, M. Ishikawa, K. Miyatani, K. Kohn, Three-dimensional magnetic ordering in the quasi-one-dimensional Ising magnet $CoNb_2O_6$ with partially released geometrical frustration, Phys. Rev. B 60 (1999) 3331–3345. doi:10.1103/PhysRevB.60.3331.

[17] C. Heid, H. Weitzel, P. Burlet, M. Winkelmann, H. Ehrenberg, H. Fuess, Magnetic phase diagrams of $CoNb_2O_6$, Physica B 234-236 (1997) 574-575, proceedings of the First European Conference on Neutron Scattering. doi:10.1016/S0921-4526(96)01189-1.

[18] P. W. C. Sarvezuk, M. A. Gusmão, J. B. M. da Cunha, O. Isnard, Magnetic behavior of the $Ni_xFe_{1-x}Nb_2O_6$ quasi-one-dimensional ystem: Isolation of Ising chains by frustration, Phys. Rev. B 86 (2012) 054435. doi:10.1103/PhysRevB.86.054435.

[19] P. W. C. Sarvezuk, E. J. Kinast, C. V. Colin, M. A. Gusmão, J. B. M. da Cunha, O. Isnard, New investigation of the magnetic structure of $CoNb_2O_6$ columbite, J. Appl. Phys. 109 (7) (2011) 07E160. doi:10.1063/1.3562516.

[20] P. W. C. Sarvezuk, E. J. Kinast, C. V. Colin, M. A. Gusmão, J. B. M. da Cunha, O. Isnard, Suppression of magnetic ordering in quasi-one-dimensional $Fe_xCo_{1-x}Nb_2O_6$ compounds, Phys. Rev. B 83 (17) (2011) 174412. doi:10.1103/PhysRevB.83.174412.

[21] L. J. de Jongh, A. R. Miedema, Experiments on simple magnetic model systems, Adv. Phys. 23, 1 (1974) 1–260. doi:10.1080/00018739700101558.

[22] F. García-Alvarado, A. Orera, J. Canales-Vázquez, J. T. S. Irvine, On the electrical properties of synthetic manganocolumbite $MnNb_2O_{6-\delta}$, Chem. Mater. 18 (16) (2006) 3827–3834. doi:10.1021/cm0603203.

[23] C. Tealdi; M. C. Mozzati; L. Malavasi; T. Ciabattoni; R. Amantea; C. B. Azzoni, Columbite-type $Fe_xMn_{1-x}Nb_2O_6$ solid solution: structural and magnetic characterization, Phys. Chem. Chem. Phys. 6 (2004) 4056-4061. doi:10.1039/b405666c.

[24] J. B. Goodenough, Magnetism and the Chemical Bond, Interscience, New York, 1963.

[25] A. P. Ramirez, Strongly Geometrically Frustrated Magnets, Annu. Rev. Mater. Sci. 24 (1994) 453-480. doi:10.1146/annurev.ms.24.080194.002321.

[26] M. Stefan, D. Ghica, S. V. Nistor, A. V. Maraloiu, R. Plugaru, Mn^{2+} ions distribution in doped sol-gel deposited ZnO films, Appl. Surf. Sci. 396 (2017) 1880-1889. doi:10.1016/j.apsusc.2016.02.167.